Eur. J. Biochem. **269**, 3831–3837 (2002) © FEBS 2002 doi:10.1046/j.1432-1033.2002.03079.x

Dissecting the effect of trifluoroethanol on ribonuclease A

Subtle structural changes detected by nonspecific proteases

Jens Köditz, Ulrich Arnold and Renate Ulbrich-Hofmann

Department of Biochemistry/Biotechnology, Martin-Luther University Halle-Wittenberg, Halle, Germany

With the aim to distinguish between local and global conformational changes induced by trifluoroethanol in RNase A, spectroscopic and activity measurements in combination with proteolysis by unspecific proteases have been exploited for probing structural transitions of RNase A as a function of trifluoroethanol concentration. At > 30% (v/v) trifluoroethanol (pH 8.0; 25 °C), circular dichroism and fluorescence spectroscopy indicate a cooperative collapse of the tertiary structure of RNase A coinciding with the loss of its enzymatic activity. In contrast to the denaturation by guanidine hydrochloride, urea or temperature, the breakdown of the tertiary structure in trifluoroethanol is accompanied by an induction of secondary structure as detected by far-UV circular dichroism spectroscopy. Proteolysis with the nonspecific proteases subtilisin Carlsberg or proteinase K, both of which attack native RNase A at the Ala20-Ser21 peptide bond, yields refined information on conformational changes, particularly in the pretransition region. While trifluoroethanol at concentrations > 40% results in a strong increase of the rate of proteolysis and new primary cleavage sites (Tyr76-Ser77, Met79-Ser80) were identified, the rate of proteolysis at trifluoroethanol concentrations < 40% (v/v) is much smaller (up to two orders of magnitude) than that of the native RNase A. The proteolysis data point to a decreased flexibility in the surrounding of the Ala20-Ser21 peptide bond, which we attribute to subtle conformational changes of the ribonuclease A molecule. These changes, however, are too marginal to alter the overall catalytic and spectroscopic properties of ribonuclease A.

Keywords: ribonuclease A; trifluoroethanol; unfolding; proteolysis: spectroscopy.

The application of organic solvents in enzymatically catalyzed reactions has gained increasing importance [1,2]. Unfortunately, most of these solvents act as a denaturant. Like conventional denaturants such as guanidine hydrochloride (GdnHCl), urea or elevated temperatures, they destroy the tertiary structure of proteins which results in the loss of enzymatic activity. Regarding the secondary structure of proteins, however, organic solvents generally differ from the aforementioned denaturants. Elements of the secondary structure, especially helices, were found to be stabilized [3], induced [4,5] or re-arranged [6,7]. Therefore, organic solvents, mainly halogenated alcohols, have also come into focus in connection with membrane mimetics [8,9], folding assistance [10] and aggregation processes [11], being important for prion proteins or Alzheimer's β-amyloid peptide [12].

Trifluoroethanol has been established as a model solvent with which to investigate structural changes in protein molecules under the influence of water-miscible organic solvents (reviewed in [13]). The reasons for its ability to propagate secondary structure, the replacement of water molecules bound to the peptide backbone by trifluoroethanol molecules, the proton donator/acceptor properties of the trifluoroethanol molecule for hydrogen bonds and the influence of trifluoroethanol on the dielectric constant of the medium, have been discussed [14]. For model peptides [3] and unfolded proteins such as disulfide reduced hen lysozyme [15], β-lactoglobulin A [6] or RNase A [16], intense helix formation was found even at low concentrations of trifluoroethanol. For folded proteins, however, an appreciable effect on the tertiary and secondary structure was found only at higher concentrations of the solvent [13]. At low concentrations of trifluoroethanol, the propagation of helical structures seems to be hampered by the still intact tertiary structure. Only after disrupting the tertiary structure of the protein, trifluoroethanol is presumed to be able to induce helical structures due to 'the need to overcome the global stability of the native fold' [13]. Despite obstructions by the still-intact tertiary structure, however, subtle changes of the secondary structure elements are conceivable even in the pretransition region of global unfolding. Such small conformational changes will not be detectable in spectroscopic equilibrium studies. Proteolysis, however, has proven to be a valuable probe for detecting local conformational changes if they are adjacent to a potential cleavage site [17]. The local accessibility and flexibility of the peptide bond is the crucial prerequisite for a successful proteolytic attack [18]. Changes in the proteolytic susceptibility of a protein therefore yield information on structural changes at the

Correspondence to R. Ulbrich-Hofmann, Martin-Luther University Halle-Wittenberg, Department of Biochemistry/Biotechnology, Kurt-Mothes-Str. 3, D-06120 Halle, Federal Republic of Germany. Fax: +49 3455527303. Tel: +49 3455524865, E-mail: ulbrich-hofmann@biochemtech.uni-halle.de

Abbreviations: GdnHCl, guanidine hydrochloride; RNase A, ribonuclease A; cCMP, cytidine 2′-3′-cytidine monophosphate.

Enzymes: proteinase K (EC 3.4.21.64); ribonuclease A (EC 3.1.27.5); subtilisin Carlsberg (EC 3.4.21.62).

Note: a web site is available at http://www.biochemtech.uni-halle.de/biotech/index.html

(Received 7 March 2002, revised 6 June 2002, accepted 25 June 2002)

respective cleavage sites [19,20]. In the present paper, we have exploited limited proteolysis with subtilisin Carlsberg and proteinase K completed by spectroscopy and activity measurements to investigate the conformational changes of RNase A (EC 3.1.27.5) under the influence of trifluoroethanol. Both proteases are able to degrade RNase A under native conditions [21–23]. With the addition of trifluoroethanol, the susceptibility of RNase A to both proteases changes considerably. Whilst global conformational changes of RNase A could also be disclosed by spectroscopy, proteolysis allowed detection of subtle local conformational changes in the pretransition region of global unfolding.

MATERIALS AND METHODS

Materials

RNase A from Sigma was purified to homogeneity on a MONO S FPLC column (Pharmacia). Subtilisin Carlsberg, proteinase K, cytochrome *c* (horse heart), soybean trypsin inhibitor and bovine pancreatic trypsin inhibitor were purchased from Sigma and used without further purification. Trifluoroethanol and cytidine 2′:3′-cyclic monophosphate (cCMP) were from Fluka, phenylmethanesulfonyl fluoride was from Merck, and *N*-succinyl-Ala-Ala-Ala-*p*-nitroanilide from Bachem. All other chemicals were the purest ones commercially available.

Determination of RNase A concentration

The protein concentration of RNase A stock solution was determined by using the molar absorption coefficient $\varepsilon = 9800\ \text{M}^{-1}\cdot\text{cm}^{-1}$ at 278 nm [24].

Spectroscopy and determination of the transition curve

CD spectroscopy was carried out on a 62-A DS CD spectrophotometer (Aviv) at 25 °C. Samples were prepared in 50 mM Tris/HCl buffer, pH 8.0, containing 0–70% (v/v) trifluoroethanol. CD spectra were recorded at an RNase A concentration of 2 $\text{mg}\cdot\text{mL}^{-1}$ using a quartz cuvette of 0.1 mm path length or 0.5 $\text{mg}\cdot\text{mL}^{-1}$ using a quartz cuvette of 1 cm path length in the far-UV (200–260 nm) and in the near-UV region (250–340 nm), respectively.

Fluorescence spectroscopy was carried out on a Fluoro-Max-2 spectrometer (Yvon-Spex) at 25 °C using a cuvette of 1 cm path length. The slit width was 1 nm for excitation at 278 nm and 10 nm for emission. Fluorescence spectra were recorded from 290 to 350 nm with a step width of 1 nm. Integration time at each wavelength was 0.5 s. Ten single spectra were averaged. The RNase A samples were 100 $\mu\text{g}\cdot\text{mL}^{-1}$ in 50 mM Tris/HCl buffer, pH 8.0, containing 0–70% (v/v) trifluoroethanol. For the transition curve, the fluorescence signal was recorded at 303 nm and averaged over 200 s. RNase A samples were 130 $\mu\text{g}\cdot\text{mL}^{-1}$ in 50 mM Tris/HCl buffer, pH 8.0, containing 0–64% (v/v) trifluoroethanol.

The fluorescence signals at 303 nm and the CD signals at 278 nm were fitted to a two-state model according to Pace *et al.* [25] by nonlinear regression. The fraction of native protein (f_N) was calculated from the fitted signals.

RNase A activity assay

RNase A activity was determined at 25 °C with cCMP as substrate. Assay mixtures were composed of 50 mM Tris/HCl buffer, pH 8.0, trifluoroethanol (0–50%, v/v), cCMP (7 mM) and RNase A (20–100 $\mu\text{g}\cdot\text{mL}^{-1}$). The reaction was followed at 286 nm in a quartz cuvette of 0.1 cm path length. Initial velocities were calculated from the linear increase of absorbance. Each value given in Fig. 4 is the average of three independent measurements ± SD.

Proteinase K activity assay

Proteinase K activity was determined at 25 °C with *N*-succinyl-Ala-Ala-Ala-*p*-nitroanilide as substrate [26]. Assay mixtures were composed of 50 mM Tris/HCl buffer, pH 8.0, $CaCl_2$ (1 mM), trifluoroethanol (0–60%, v/v), *N*-succinyl-Ala-Ala-Ala-*p*-nitroanilide (1 mM) and proteinase K (2.5–20 $\mu\text{g}\cdot\text{mL}^{-1}$). The reaction was followed at 410 nm in a cuvette of 1 cm path length. Initial velocities were calculated from the linear increase of absorbance. Each value given in Fig. 1 is the average of three independent measurements ± SD.

Trifluoroethanol-induced denaturation and proteolysis

Limited proteolysis of RNase A was performed in 50 mM Tris/HCl buffer, pH 8.0, containing $CaCl_2$ (1 mM) and trifluoroethanol (0–60%, v/v) at 25 °C. To 160 μL of this solution were added 20 μL of protease solution [subtilisin Carlsberg (40 $\mu\text{g}\cdot\text{mL}^{-1}$) or proteinase K (0.02–10 $\text{mg}\cdot\text{mL}^{-1}$) in 50 mM Tris/HCl buffer, pH 8.0, containing 10 mM $CaCl_2$] and 20 μL RNase A (2 $\text{mg}\cdot\text{mL}^{-1}$ in 50 mM Tris/HCl buffer, pH 8.0). After defined time intervals, samples of 10 μL were rapidly removed, mixed with 13 μL of a stopping solution (1 mL of 50 mM phenylmethanesulfonyl fluoride in 2-propanol and 300 μL 0.1 M HCl), and heated at 95 °C for 10 min. After cooling, the samples were neutralized by addition of 3 μL 0.1 M NaOH.

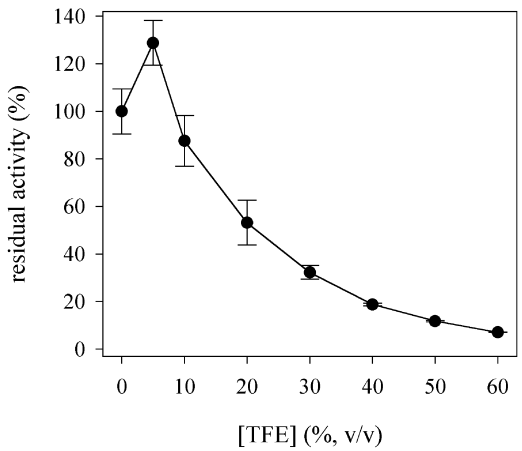

Fig. 1. Activity of proteinase K as a function of the concentration of trifluoroethanol. Activity of proteinase K was determined with *N*-succinyl-Ala-Ala-Ala-*p*-nitroanilide as substrate at 25 °C as described in Materials and methods.

RP-HPLC of the proteolytic fragments

Reduction of the disulfide bonds was performed in 50 mM Tris/HCl buffer, pH 8.0, containing 1,4-dithiothreitol (10 mM) and GdnHCl (5 M) for 2 h. Afterwards, the SH groups were carbamidomethylated by treatment with 100 mM iodoacetamide for 15 min. Both reactions were performed in the dark under nitrogen at room temperature. Protein fragments were separated on an inert HPLC system (Merck-Hitachi) using a C_8 reverse-phase column (Vydac). The solvent gradient was produced from degassed HPLC-grade water containing 0.07% trifluoroacetic acid and degassed acetonitrile containing 0.056% trifluoroacetic acid. The flow rate was 1.0 $mL \cdot min^{-1}$. Absorbance was followed at 214 nm and fractions for protein sequencing and MALDI-MS were collected manually.

MALDI-MS and N-terminal protein sequencing

MALDI-MS was carried out as described previously [27] on a reflectron-type time-of-flight mass spectrometer Reflex™ (Bruker-Franzen, Bremen, Germany). Amino acid sequences were determined using the protein sequencer 476 A (Applied Biosystems, Foster City, CA, USA) according to the manufacturer's instructions.

Electrophoresis and densitometric evaluation

Electrophoresis was carried out under reducing conditions on a Midget electrophoresis unit (Hoefer) according to Schägger & von Jagow [28] but using 10% and 18% (w/v) acrylamide for sampling and separation gels without spacer gel. Silver staining of the SDS/PAGE gels was performed according to Blum *et al.* [29]. For densitometric evaluation of the band of intact RNase A, the SDS/PAGE gels were stained with Coomassie brilliant blue G 250 and scanned at 595 nm using a CD 60 densitometer (Desaga).

Rate constants of proteolysis and relative proteolytic susceptibility

The rate constants of proteolysis (k_p) were calculated from the time-dependent decrease of the peak areas of intact RNase A in the scanned SDS/PAGE gels, which followed a first-order reaction. Due to the wide range of k_p values it was not possible to determine k_p at a constant concentration of proteinase K for all concentrations of trifluoroethanol. Therefore, k_p was determined as a function of the concentration of proteinase K for each concentration of trifluoroethanol (see 'Trifluoroethanol-induced denaturation and proteolysis'). The k_p values were found to increase linearly with the increase of the protease concentration. The slopes of these linear functions (k_p vs. proteinase K concentration) were corrected by the proteinase K activity for each trifluoroethanol concentration (Fig. 1) to eliminate the influence of changes of the protease activity on k_p. The relative proteolytic susceptibility given in Fig. 4 was obtained by relating these values to the value determined for 0% trifluoroethanol.

Analytical ultracentrifugation

Analytical ultracentrifugation was carried out on a Beckman Optima XL-A ultracentrifuge at 20 °C according to the manufacturer's instructions. Protein concentration was adjusted to 0.7 $mg \cdot mL^{-1}$ in 20 mM Tris/HCl buffer, pH 8.0, containing 0 or 20% trifluoroethanol, respectively.

RESULTS

Spectroscopy

To dissect changes of the secondary and tertiary structure of RNase A in the presence of trifluoroethanol, CD spectra in the near- and far-UV regions were recorded at trifluoroethanol concentrations of between 0 and 70% (Fig. 2). In the near-UV region, characterizing the tertiary structure, no noticeable changes were observed at concentrations of up to 30% trifluoroethanol. Above 30% trifluoroethanol, the spectra revealed that the tertiary structure was increasingly disturbed. At 50% trifluoroethanol, the tertiary structure was fully disrupted, and the CD signal remained unchanged at even higher trifluoroethanol concentrations (Fig. 2A). From the respective CD signals at 278 nm a transition curve was constructed (Fig. 4). As an alternative approach to detect changes of the tertiary structure, we recorded fluorescence spectra of RNase A in 0–70% (v/v) trifluoroethanol (Fig. 3). Both the slight shift of the emission maximum to a shorter wavelength and the strong increase of the fluorescence signal indicate changes of the tertiary structure of the RNase A molecule. Furthermore, fluorescence emission of RNase A at 303 nm was followed as a

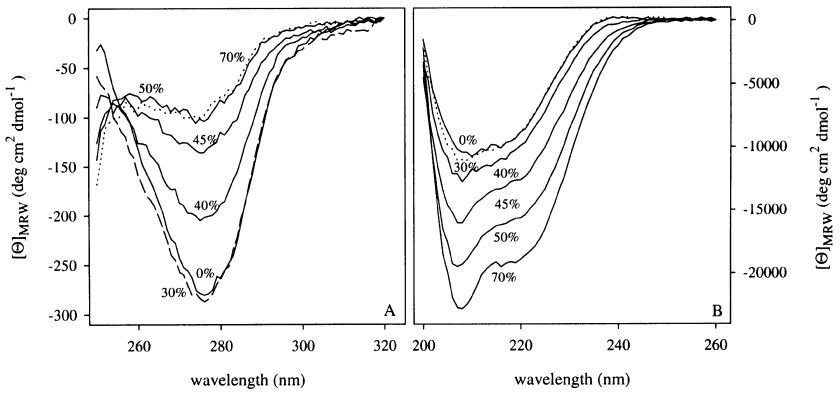

Fig. 2. Near-UV (A) and far-UV (B) CD spectra of RNase A in trifluoroethanol. RNase A was dissolved in 50 mM Tris/HCl, pH 8.0, in the absence of trifluoroethanol and in the presence of 30, 40, 45, 50 and 70% (v/v) trifluoroethanol. CD spectra were recorded as described in Materials and methods.

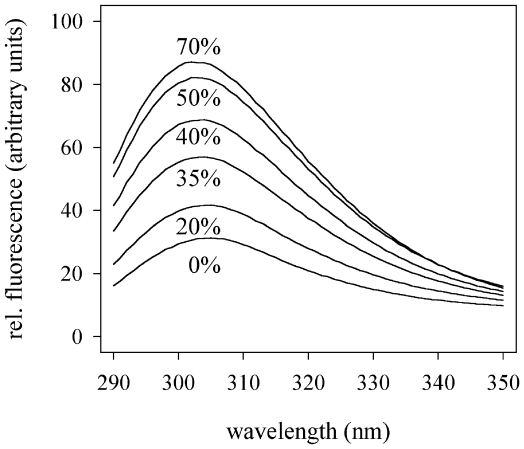

Fig. 3. Fluorescence spectra of RNase A in trifluoroethanol. RNase A was dissolved in 50 mM Tris/HCl, pH 8.0, in the absence of trifluoroethanol and in the presence of 20, 35, 40, 50 and 70% (v/v) trifluoroethanol. Fluorescence spectra were recorded as described in Materials and methods.

function of the concentration of trifluoroethanol. The respective transition curve coincides with that obtained from CD measurements (Fig. 4).

As found for near-UV CD spectra, no changes were detected in the far-UV CD spectra for concentrations up to 30% trifluoroethanol. Above 30% trifluoroethanol, an increase of the negative ellipticity in the far-UV region indicates the induction of additional secondary structure (mainly helical structures) (Fig. 2B). However, no pronounced transition could be detected and the process was not completed at 70% trifluoroethanol.

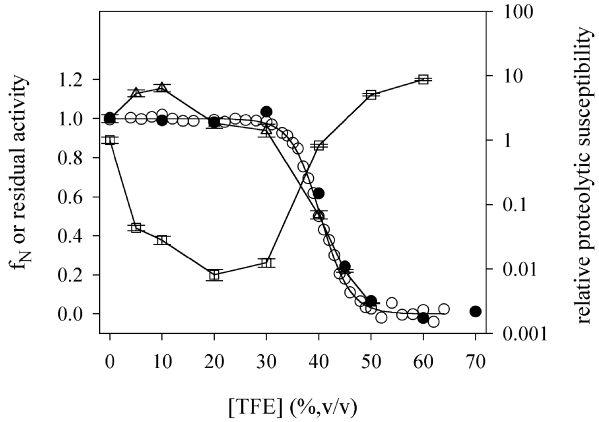

Fig. 4. Conformational changes of RNase A as a function of trifluoroethanol concentration followed by fluorescence and CD spectroscopy, activity measurements and proteolysis. f_N represents the fraction of native protein as determined by fluorescence spectroscopy at 303 nm (○) or by CD spectroscopy at 278 nm (●) at 25 °C. Residual activity of RNase A (△) was determined with cCMP as substrate. The relative proteolytic susceptibility of RNase A towards proteinase K (□) was obtained from first-order rate constants of proteolysis (k_p) as described in Materials and methods.

To gain insight into the changes detected by proteolysis (see below), we investigated RNase A in the absence and presence of 20% trifluoroethanol by NOESY and TOCSY NMR spectroscopy. However, due to the high pH value (8.0) and the high flexibility of the loop region of interest (around Ala20) the signal was very weak and no assignment to the protein sequence was possible.

RNase A activity

To determine whether the differences in the changes of the tertiary and secondary structures are reflected in the activity of RNase A, its activity towards cCMP was measured as a function of the concentration of trifluoroethanol (Fig. 4). While the decrease of RNase A activity above 30% trifluoroethanol coincides with the disruption of the tertiary structure, a slight activation of RNase A was observed at low concentrations of trifluoroethanol.

Proteolytic susceptibility of RNase A

Fragmentation of RNase A by proteinase K and subtilisin Carlsberg. The proteolytic susceptibility of RNase A to proteinase K and subtilisin Carlsberg as a function of the concentration of trifluoroethanol was analysed by SDS/PAGE. In Fig. 5, typical proteolytic fragment patterns of RNase A emerging in 0, 20 and 40% trifluoroethanol (v/v) as a function of time are shown. Under native conditions, proteinase K and subtilisin Carlsberg efficiently cleave RNase A at the peptide bond Ala20-Ser21 [21,22] yielding the so-called RNase S. The large fragment of RNase S (residues 21–124), called S-protein, is visible in the SDS/PAGE gel (Fig. 5B). Surprisingly, in 20% trifluoroethanol no fragmentation of RNase A by both proteases was observed (Fig. 5C), whereas in 40% trifluoroethanol, again a degradation of RNase A was detected (Fig. 5D). In contrast to native conditions where only the S-protein was observed, various fragments were found in 40% trifluoroethanol. The same trend of proteolytic susceptibility of

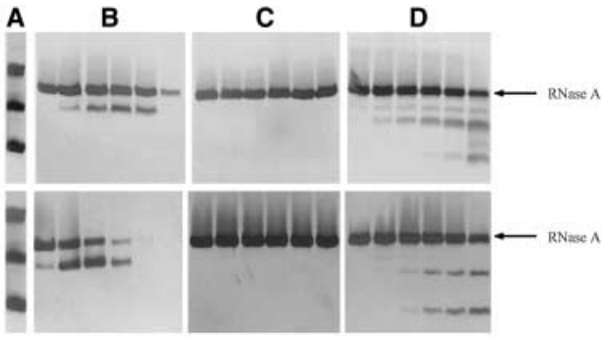

Fig. 5. Time course of the proteolytic degradation of RNase A by subtilisin Carlsberg (upper panel) and proteinase K (lower panel) in trifluoroethanol. RNase A was incubated in the presence of subtilisin Carlsberg or proteinase K at a ratio of 50 : 1 (w/w) in (B) 0% (C) 20%, and (D) 40% trifluoroethanol (v/v) at 25 °C. The reaction was stopped after 30 s, 10 min, 30 min, 1 h, 2 h and 6 h (from left to right in each SDS/PAGE gel). Lane (A) shows the reference proteins soybean trypsin inhibitor (21 kDa), cytochrome *c* (12.4 kDa) and bovine pancreatic trypsin inhibitor (6.5 kDa).

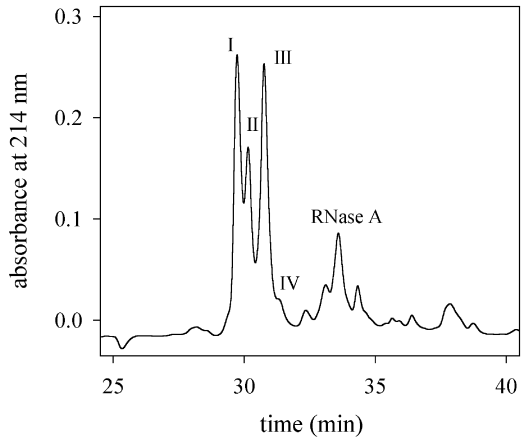

Fig. 6. RP-HPLC separation of RNase A fragments. RNase A was treated with subtilisin (50 : 1, w/w) in 50% trifluoroethanol at 25 °C for 2 h and subsequently treated as described in Materials and methods.

RNase A was found with elastase (results not shown) but due to the low stability of elastase in higher concentrations of trifluoroethanol, we did not investigate further with this protease.

To characterize the fragments of RNase A observed after proteolysis at higher concentrations of trifluoroethanol (40%), samples were analysed by RP-HPLC, MALDI-MS and N-terminal protein sequencing. A typical RP-HPLC chromatogram for the proteolytic digestion of RNase A by subtilisin Carlsberg is shown in Fig. 6. The results for subtilisin and proteinase K are summarized in Table 1. For both proteases the same four fragments could be found: the N-terminal fragments 1–76 and 1–79 and the complementary C-terminal fragments 77–124 and 80–124. Thus, the peptide bonds 76–77 and 79–80 of RNase A were identified as cleavage sites which become first accessible under denaturation by trifluoroethanol ('primary cleavage sites'). Due to the low concentration, the fragment with the highest molecular mass in Fig. 5D, upper panel, could not be characterized. According to its behaviour in electrophoresis, it probably represents fragment 21–124, as in Fig. 5A.

Quantification of the proteolytic susceptibility of RNase A. To gain further insight into the changes of the proteolytic susceptibility of RNase A as a function of trifluoroethanol concentration, the proteolytic degradation by proteinase K was quantified at 0–60% trifluoroethanol. From the decrease of the RNase A band in SDS/PAGE gels as a function of time, rate constants of proteolysis were determined, converted into the (protease-concentration independent) proteolytic susceptibility, and corrected for differences in proteolytic activity as described in Materials and methods. Figure 4 demonstrates that differences in the proteolytic susceptibility range three orders of magnitude with k_p under native conditions being $(9.7 \pm 0.7) \times 10^{-3}\ s^{-1}$ (at 100 $\mu g \cdot mL^{-1}$ proteinase K). While above 30% trifluoroethanol the proteolytic susceptibility of RNase A strongly increases, which coincides with the disruption of the tertiary structure of the RNase A molecule, in 20% trifluoroethanol the proteolytic susceptibility is reduced by two orders of magnitude (Fig. 4).

To test whether aggregation of RNase A in 20% trifluoroethanol is the reason for the decrease of k_p, we applied respective samples to ultracentrifugation (not shown). The results unambiguously confirm that RNase A solely exists as soluble monomer under these conditions.

DISCUSSION

Whilst global unfolding significantly changes the spectroscopic properties of a protein, the detection of subtle conformational changes of the protein structure, which can already occur clearly before global unfolding, is more challenging. In this paper we investigated the influence of trifluoroethanol on the conformation of RNase A with particular consideration of the pretransition region of global unfolding.

In correspondence to reports by other authors [16,30,31], CD spectra in the near-UV region, as well as fluorescence signals, unveil the disruption of the tertiary structure of RNase A in > 30% trifluoroethanol. CD spectra in the far-UV region, on the other hand, indicate a detectable increase in the content of secondary structure only after the disruption of the native tertiary structure of RNase A (Figs 2–4). Interestingly, the preservation of the tertiary structure coincides with the activity profile of RNase A (Fig. 4). This behaviour differs from that reported for the denaturation by GdnHCl or temperature [20], where the decrease of the activity of RNase A precedes the disruption of the tertiary structure. Apart from a slight activation, an effect which was also reported for other enzymes in the presence of various solvents [32], low concentrations of

Table 1. N-Terminal sequences and molecular masses of RNase A fragments obtained by limited proteolysis with subtilisin or proteinase K. RNase A was treated with subtilisin or proteinase K (50 : 1, w/w) in 50% trifluoroethanol (v/v) at 25 °C for 2 h or 1 h, respectively, and analysed by RP-HPLC, protein sequencing and MALDI-MS as described in Materials and methods. The fraction numbers correspond to those in Fig. 6. [a]N-Terminal sequencing was performed for fragments generated by digestion of RNase A by subtilisin Carlsberg only.

Fraction	N-Terminal sequence determined by protein sequencing[a]	Assigned RNase A sequence	Molecular mass determined by MALDI-MS (Da)		Suggested RNase fragment	
			Subtilisin	Proteinase K	Sequence	Molecular mass (Da)
I	Ser-Ile-Thr-Asp	80–83	5087	5088	80–124	5088
II	Ser-Thr-Met-Ser	77–80	5407	5408	77–124	5407
III	Lys-Glu-Thr-Ala	1–4	8758	8760	1–76	8758
IV	Lys-Glu-Thr-Ala	1–4	9079	9079	1–79	9077

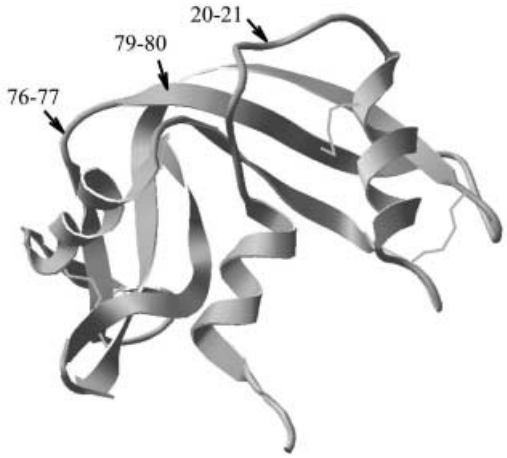

Fig. 7. Tertiary structure of RNase A. The model was taken from the Brookhaven protein data bank and drawn with PDBViewer. α Helices and β sheets are presented as ribbons and sites of proteolytic attack are indicated by arrows.

trifluoroethanol seem to have no impact on the activity of RNase A.

Limited proteolysis by unspecific proteases resulted in more detailed information on conformational changes of RNase A in trifluoroethanol. In the absence of trifluoroethanol, subtilisin Carlsberg and proteinase K degrade RNase A by primarily cleaving the Ala20-Ser21 peptide bond (Figs 5B and 7 [21,22]). This cleavage is possibly due to the high flexibility of the loop region around this peptide bond [33], whereas the rest of the RNase A molecule is not accessible enough to be attacked. With the addition of trifluoroethanol, alterations of the susceptibility of RNase A toward proteolysis and changes of the proteolytic fragment patterns occur. The lack of proteolytic fragments in 5–30% trifluoroethanol (Fig. 5C) is caused by the drastically decreased rate of primary cleavage of RNase A (Fig. 4), as discussed below. As a consequence of the breakdown of the tertiary structure of RNase A in concentrations of trifluoroethanol > 30%, new primary cleavage sites (Tyr76-Ser77, Met79-Ser80) become accessible (Fig. 5D, Table 1). These peptide bonds are located in a bulge and a β strand [34] (Fig. 7) which belongs to the core of the RNase A and is not accessible under native conditions [35]. In comparison with the denaturation by GdnHCl or temperature [20], however, a fewer number of new primary cleavage sites arise in denaturation by trifluoroethanol. This result reflects the different content of secondary structure in the denatured state of RNase A, which decreases in the order trifluoroethanol > temperature [36] > GdnHCl [37]. In accordance with the emergence of new primary cleavage sites, the proteolytic susceptibility of RNase A increases dramatically at high trifluoroethanol concentrations (Fig. 4).

As reasons for the strong decrease of the proteolytic susceptibility of the RNase A molecule to proteinase K in 5–30% trifluoroethanol, aggregation of the protein, as reported for creatine kinase [38], and activity changes of the protease, could be ruled out. It is noteworthy that in this range of trifluoroethanol concentration, no significant changes of the spectroscopic properties of the enzyme could be detected. Therefore, the decrease of the proteolytic susceptibility has to be attributed to a decreased (local) flexibility of the RNase A molecule at the loop region around Ala20 which is located between helices I and II of RNase A [34]. For the isolated fragment 1–19 of RNase A, helix formation with the addition of low concentrations of trifluoroethanol has been reported [39,40], as well as for fragments 21–42 [41] and 50–61 [42] resembling helices II and III, respectively, of RNase A. As a consequence, we propose that subtle changes of confined regions (e.g. at the ends of the helices) brought about by trifluoroethanol result in a rigidity of the loop and, hence, to a proteolytically less susceptible state of the RNase A molecule without affecting the overall structure of the protein. Interestingly, the stabilization of RNase A toward subtilisin and proteinase K by 20% trifluoroethanol is similar to that caused by the substitution of Ala20 with Pro [23]. While the helix-forming effect is well known for both peptides [3] and unfolded proteins [16], trifluoroethanol-induced propagation of secondary structure in a natively folded protein is described here for the first time.

ACKNOWLEDGEMENTS

We thank Dr A. Schierhorn and Dr H. Lilie, Martin-Luther University Halle, Germany, for performing MALDI-MS and analytical ultracentrifugation measurements. We thank Dr K.-P. Rücknagel, Max-Planck Forschungsstelle 'Enzymologie der Peptidbindung', Halle, Germany, for performing N-terminal protein sequencing. We thank Dr P. Bayer, Max-Planck Institute of Molecular Physiology, Dortmund, Germany, for performing NMR spectroscopy experiments. The support for Jens Köditz by the Land Sachsen-Anhalt and by the Max-Buchner-Forschungsstiftung, Frankfurt/Main, Germany, is gratefully acknowledged.

REFERENCES

1. Dordick, J.S. (1991) Enzymatic catalysis in organic media: fundamentals and selected applications. *ASGSB Bull.* **4**, 125–132.
2. Melo, E.P., Aires-Barros, M.R. & Cabral, J.M. (2001) Reverse micelles and protein biotechnology. *Biotechnol. Annu. Rev.* **7**, 87–129.
3. Luo, P. & Baldwin, R.L. (1997) Mechanism of helix induction by trifluoroethanol: a framework for extrapolating the helix-forming properties of peptides from trifluoroethanol/water mixtures back to water. *Biochemistry* **36**, 8413–8421.
4. Mizuno, K., Kaido, H., Kimura, K., Miyamoto, K., Yoneda, N., Kawabata, T., Tsurusaki, T., Hashizume, N. & Shindo, Y. (1984) Studies of the interaction between alcohols and amides to identify the factors in the denaturation of globular proteins in haloalcohol + water mixtures. *J. Chem. Soc., Faraday Trans.* **1**, 879–894.
5. Uversky, V.N., Narizhneva, N.V., Kirschstein, S.O., Winter, S. & Lober, G. (1997) Conformational transitions provoked by organic solvents in beta-lactoglobulin: can a molten globule like intermediate be induced by the decrease in dielectric constant? *Fold. Des.* **2**, 163–172.
6. Shiraki, K., Nishikawa, K. & Goto, Y. (1995) Trifluoroethanol-induced stabilization of the alpha-helical structure of beta-lactoglobulin: implication for non-hierarchical protein folding. *J. Mol. Biol.* **245**, 180–194.
7. Liu, Z.P., Rizo, J. & Gierasch, L.M. (1994) Equilibrium folding studies of cellular retinoic acid binding protein, a predominantly beta-sheet protein. *Biochemistry* **33**, 134–142.
8. Mukhopadhyay, K. & Basak, S. (1998) Conformation induction in melanotropic peptides by trifluoroethanol: fluorescence and circular dichroism study. *Biophys. Chem.* **74**, 175–186.

9. Yoon, M.K., Park, S.H., Won, H.S., Na, D.S. & Lee, B.J. (2000) Solution structure and membrane-binding property of the N-terminal tail domain of human annexin I. *FEBS Lett.* **484**, 241–245.
10. Hamada, D., Chiti, F., Guijarro, J.I., Kataoka, M., Taddei, N. & Dobson, C.M. (2000) Evidence concerning rate-limiting steps in protein folding from the effects of trifluoroethanol. *Nat. Struct. Biol.* **7**, 58–61.
11. Chiti, F., Webster, P., Taddei, N., Clark, A., Stefani, M., Ramponi, G. & Dobson, C.M. (1999) Designing conditions for *in vitro* formation of amyloid protofilaments and fibrils. *Proc. Natl Acad. Sci. USA* **96**, 3590–3594.
12. Cohen, F.E. & Prusiner, S.B. (1998) Pathologic conformations of prion proteins. *Annu. Rev. Biochem.* **67**, 793–819.
13. Buck, M. (1998) Trifluoroethanol and colleagues: cosolvents come of age. Recent studies with peptides and proteins. *Q. Rev. Biophys.* **31**, 297–355.
14. Rajan, R. & Balaram, P. (1996) A model for the interaction of trifluoroethanol with peptides and proteins. *Int. J. Pept. Protein Res.* **48**, 328–336.
15. Yang, J.J., Buck, M., Pitkeathly, M., Kotik, M., Haynie, D.T., Dobson, C.M. & Radford, S.E. (1995) Conformational properties of four peptides spanning the sequence of hen lysozyme. *J. Mol. Biol.* **252**, 483–491.
16. Sivaraman, T., Kumar, T.K., Hung, K.W. & Yu C. (1999) Influence of disulfide bonds on the induction of helical conformation in proteins. *J. Protein Chem.* **18**, 481–488.
17. Price, N.C. & Johnson, C.M. (1990) Proteinases as probes of conformation of soluble proteins. In *Proteolytic Enzymes. A Practical Approach* (Beynon, R.J. & Bond, J.S., eds), pp. 163–180. IRL Press, Oxford.
18. Hubbard, S.J. (1998) The structural aspects of limited proteolysis of native proteins. *Biochim. Biophys. Acta* **1382**, 191–206.
19. Arnold, U., Rücknagel, K.P., Schierhorn, A. & Ulbrich-Hofmann, R. (1996) Thermal unfolding and proteolytic susceptibility of ribonuclease A. *Eur. J. Biochem.* **237**, 862–869.
20. Arnold, U. & Ulbrich-Hofmann, R. (2000) Differences in the denaturation behavior of ribonuclease A induced by temperature and guanidine hydrochloride. *J. Protein Chem.* **19**, 345–352.
21. Richards, F.M. & Vithayathil, P.J. (1959) The preparation of subtilisin-modified ribonuclease and the separation of the peptide and protein components. *J. Biol. Chem.* **234**, 1459–1465.
22. Rauber, N.R., Jany, K.D. & Pfleiderer, G. (1978) Ribonuclease A digestion by proteinase K. *Z. Naturforsch.* **C33**, 660–663.
23. Markert, Y., Köditz, J., Mansfeld, J., Arnold, U. & Ulbrich-Hofmann, R. (2001) Increased proteolytic resistance of ribonuclease A by protein engineering. *Protein Eng.* **14**, 791–796.
24. Sela, M. & Anfinsen, C.B. (1957) Some spectrophotometric and polarimetric experiments with ribonuclease. *Biochim. Biophys. Acta* **24**, 229–235.
25. Pace, C.N., Shirley, B.A. & Thomson, J.A. (1989) Measuring the conformational stability of a protein. In *Protein Structure – a Practical Approach* (Creighton, T.E., ed.), pp. 331–330. IRL Press, Oxford.
26. Peters, K., Pauli, D., Hache, H., Boteva, R.N., Genov, N.C. & Fittkau, S. (1989) Subtilisin DY – kinetic characterization and comparison with related proteinases. *Curr. Microbiol.* **18**, 171–177.
27. Arnold, U., Schierhorn, A. & Ulbrich-Hofmann, R. (1998) Influence of the carbohydrate moiety on the proteolytic cleavage sites in ribonuclease B. *J. Protein Chem.* **17**, 397–405.
28. Schägger, H. & von Jagow, G. (1987) Tricine-sodium dodecyl sulfate-polyacrylamide gel electrophoresis for the separation of proteins in the range from 1 to 100 kDa. *Anal. Biochem.* **166**, 368–379.
29. Blum, H., Beier, H. & Gross, J.H. (1987) Improved silver staining of plant proteins, RNA and DNA in polyacrylamide gels. *Electrophoresis* **8**, 93–99.
30. Polverino de Laureto, P., Scaramella, E., De Filippis, V., Bruix, M., Rico, M. & Fontana, A. (1997) Limited proteolysis of ribonuclease A with thermolysin in trifluoroethanol. *Protein Sci.* **6**, 860–872.
31. Gast, K., Zirwer, D., Müller-Frohne, M. & Damaschun, G. (1999) Trifluoroethanol-induced conformational transitions of proteins: insights gained from the differences between alpha-lactalbumin and ribonuclease A. *Protein Sci.* **8**, 625–634.
32. Ulbrich-Hofmann, R. & Selisko, B. (1993) Soluble and immobilized enzymes in water-miscible organic solvents: glucoamylase and invertase. *Enzyme Microb. Technol.* **15**, 33–41.
33. Santoro, J., Gonzalez, C., Bruix, M., Neira, J.L., Nieto, J.L., Herranz, J. & Rico, M. (1993) High-resolution three-dimensional structure of ribonuclease A in solution by nuclear magnetic resonance spectroscopy. *J. Mol. Biol.* **229**, 722–734.
34. Wlodawer, A., Bott, R. & Sjolin, L. (1982) The refined crystal structure of ribonuclease A at 2.0 Å resolution. *J. Biol. Chem.* **257**, 1325–1332.
35. Kiefhaber, T. & Baldwin, R.L. (1996) Hydrogen exchange and the unfolding pathway of ribonuclease A. *Biophys. Chem.* **59**, 351–356.
36. Navon, A., Ittah, V., Laity, J.H., Scheraga, H.A., Haas, E. & Gussakovsky, E.E. (2001) Local and long-range interactions in the thermal unfolding transition of bovine pancreatic ribonuclease A. *Biochemistry* **40**, 93–104.
37. Takeda, K., Sasa, K., Nagao, M. & Batra, P.P. (1988) Secondary structural changes of non-reduced and reduced ribonuclease A in solutions of urea, guanidine hydrochloride and sodium dodecyl sulfate. *Biochim. Biophys. Acta* **957**, 340–344.
38. Huang, K., Park, Y.D., Cao, Z.F. & Zhou, H.M. (2001) Reactivation and refolding of rabbit muscle creatine kinase denatured in 2,2,2-trifluoroethanol solutions. *Biochim. Biophys. Acta* **1545**, 305–313.
39. Nelson, J.W. & Kallenbach, N.R. (1986) Stabilization of the ribonuclease S-peptide alpha-helix by trifluoroethanol. *Proteins* **1**, 211–217.
40. Storrs, R.W., Truckses, D. & Wemmer, D.E. (1992) Helix propagation in trifluoroethanol solutions. *Biopolymers* **32**, 1695–1702.
41. Jiménez, M.A., Rico, M., Herranz, J., Santoro, J. & Nieto, J.L. (1988) ^{1}H-NMR assignment and folding of the isolated ribonuclease 21–42 fragment. *Eur. J. Biochem.* **175**, 101–109.
42. Jiménez, M.A., Nieto, J.L., Herranz, J., Rico, M. & Santoro, J. (1987) ^{1}H NMR and CD evidence of the folding of the isolated ribonuclease 50–61 fragment. *FEBS Lett.* **221**, 320–324.